Large-amplitude internal waves in a thermally stratified reservoir: modeling and field observations in South Baikal

Alexander A. Chesnokov

joint work with V.Yu. Liapidevskii, V.E. Ermishina and I.A. Aslamov

Lavrentyev Institute of Hydrodynamics, Novosibirsk, Russia

Conference “Dynamics in Siberia”

Novosibirsk, March 2 – 6, 2026

Introduction

Variations in seawater temperature and salinity stratify the water column, producing conditions where density disturbances can propagate as internal waves. Examples of recorded IWs; wind-driven IWs (seiches).

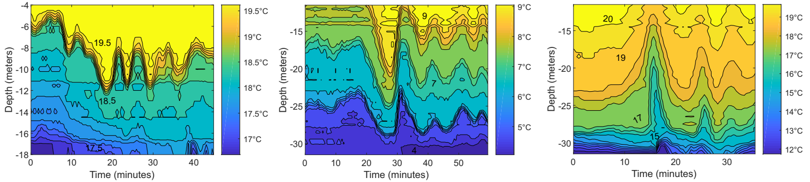

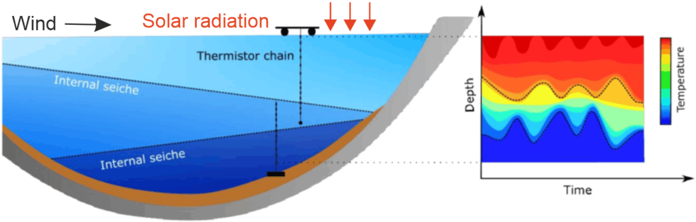

Study of nonlinear internal waves:

- Field observations of ISWs (Moum et al., 2003; Lamb & Farmer, 2011; Preusse et al., 2012; Dorostkar & Boegman, 2013; Lien et al., 2014; Zhang & Alford, 2015; Bourgault et al., 2016; Chang et al., 2021; Cyriac et al., 2023; Kozlov et al., 2023; Sun et al., 2024; Aslamov et al.; Morozov, Makarenko et al; Liapidevskii et al.; ...).
- Laboratory experiments and numerical simulation (Grue et al., 1999; Horn et al., 2001; Chen, 2007; Chen et al, 2008; Fructus et al., 2009; Aghsaee et al., 2011; Carr et al., 2011, 2017; Grace et al., 2019; Zou et al. 2020; Zhao et al., 2020; de Carvalho Bueno et al., 2021; 2023; Marcovic & Armenio, 2022; Nian et al., 2023; Zheng et al., 2024; Ermanyuk, Gavrilov, Makridin & Shmakova et al.; ...).
- Theoretical study and modelling of ISWs (Choi & Camassa, 1999; Choi, 2000; Rusås & Grue, 2002; Barros et al., 2007; 2020; Forgia & Sciortino, 2021; Derzho, 2022; Tseluiko et al., 2023; Zhao et al., 2023; Zhang et al., 2026; Makarenko et al.; Chesnokov & Liapidevskii; ...).

Mathematical model

A model describing large-amplitude long waves in a multilayer stratified fluid was derived by Choi, 2000. Due to the complexity, its application is limited to classes of 2-layer (Choi & Camassa, 1999) and 3-layer (Barros et al., 2020) flows. To simplify the multilayer model, we assume:

- the rigid-lid approximation;
- non-hydrostatic effects are taken only in the outer layers;
- the Boussinesq approximation $(0 < (\rho_i - \rho_1)/\rho_1 \ll 1)$ is applied.

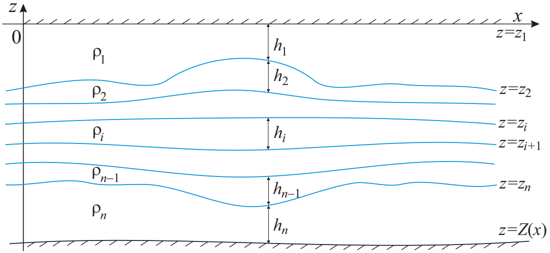

Under the above assumptions, the Choi equations take the form (Liapidevskii et al, 2020; 2021; 2023)

$$
\begin{aligned}
&\frac{\partial h_i}{\partial t} + \frac{\partial u_i h_i}{\partial x} = 0, \quad i = 1, ..., n \\
&\frac{\partial u_1}{\partial t} + \frac{\partial}{\partial x}\left(\frac{u_1^2}{2} + p\right) + \frac{\beta_1}{3h_1}\frac{\partial}{\partial x}\left(h_1^2 \frac{d_1^2 h_1}{dt^2}\right) = f_1, \\
&\frac{\partial u_i}{\partial t} + \frac{\partial}{\partial x}\left(\frac{u_i^2}{2} + p_i\right) = f_i, \quad i = 2, ..., n-1 \\
&\frac{\partial u_n}{\partial t} + \frac{\partial}{\partial x}\left(\frac{u_n^2}{2} + p_n\right) + \frac{\beta_n}{3h_n}\frac{\partial}{\partial x}\left(h_n^2 \frac{d_n^2 h_n}{dt^2}\right) = f_n.
\end{aligned}
\tag{1}
$$

Here h_i and u_i are the thickness and velocity; $d_k/dt = \partial_t + u_k \partial_x$ $(k = 1, n)$; $b_i = g(\rho_i - \rho_1)/\rho_1$ is the buoyancy; $\beta_k = 1$ or $\beta_k = 0$; p is the specific pressure at $z = 0$, and p_i have the form

$$
p_i = p + \sum_{j=2}^{i-1} b_j h_j + b_i \sum_{j=i}^{n} h_j + b_i Z.
$$

The variables f_i are

$$f_1 = -\frac{c_l}{h_1}(u_1 - u_2)|u_1 - u_2| \pm \frac{u_*^2}{h_1}, \quad f_n = -\frac{c_l}{h_n}(u_n - u_{n-1})|u_n - u_{n-1}|,$$
$$f_i = -\frac{c_l}{h_i}\Big((u_i - u_{i-1})|u_i - u_{i-1}| + (u_i - u_{i+1})|u_i - u_{i+1}|\Big),$$

where c_l is the friction at interfaces $z = z_i$, and u_* is the friction velocity of the wind.
The geometric constraint and mass balance equations give

$$\sum_{i=1}^{n} h_i = H(x) = -Z(x), \quad \sum_{i=1}^{n} u_i h_i = Q(t).$$

Direct calculations show that in terms of the functions

$$\bar{K} = u_1 - \frac{\beta_1}{3h_1}\frac{\partial}{\partial x}\Big(h_1^3\frac{\partial u_1}{\partial x}\Big), \ \bar{R} = u_n - \frac{\beta_n}{3h_n}\frac{\partial}{\partial x}\Big(h_n^3\frac{\partial u_n}{\partial x}\Big),$$

the momentum equations in system (1) for the outer layers take the form:

$$\frac{\partial \bar{K}}{\partial t} + \frac{\partial}{\partial x}\left(u_1 \bar{K} - \frac{u_1^2}{2} + p - \frac{\beta_1 h_1^2}{2}\left(\frac{\partial u_1}{\partial x}\right)^2\right) = f_1,$$
$$\frac{\partial \bar{R}}{\partial t} + \frac{\partial}{\partial x}\left(u_n \bar{R} - \frac{u_n^2}{2} + p_n - \frac{\beta_n h_n^2}{2}\left(\frac{\partial u_n}{\partial x}\right)^2\right) = f_n.$$

Numerical algorithm (Le Metayer et al, 2010). We eliminate p in the momentum equations introducing the relative velocities $s_i = u_{i+1} - u_i$ $(i = 2, ..., n-2)$ and variables $K = \bar{K} - u_2$, $R = \bar{R} - u_{n-1}$. We note that

$$u_2 = \frac{\psi - u_1 h_1 - u_n h_n}{H - h_1 - h_n}, \quad u_{n-1} = u_2 + \sum_{j=2}^{n-2} s_j, \quad \left(\psi = Q - \sum_{i=3}^{n-1} h_i \sum_{j=2}^{i-1} s_j\right),$$

i.e. u_2 and u_{n-1} are expressed through u_1, u_n, h_i, and $s_2, ..., s_{n-2}$.

For $2n-2$ unknowns $\boldsymbol{U} = (h_1, ..., h_{n-1}, K, s_2, ..., s_{n-2}, R)$ we have the following system, divided into "hyperbolic" and elliptical parts:

$$
\begin{cases}
\dfrac{\partial h_i}{\partial t} + \dfrac{\partial}{\partial x}(u_i h_i) = 0, \quad i = 1, ..., n-1 \\
\dfrac{\partial K}{\partial t} + \dfrac{\partial}{\partial x}\left(u_1 K - \dfrac{(u_1 - u_2)^2}{2} - \varphi_1 - \dfrac{\beta_1 h_1^2}{2}\Big(\dfrac{\partial u_1}{\partial x}\Big)^2\right) = f_1 - f_2, \\
\dfrac{\partial s_i}{\partial t} + \dfrac{\partial}{\partial x}\left(\dfrac{(u_{i+1} + u_i)s_i}{2} + \varphi_i\right) = f_{i+1} - f_i, \quad i = 2, ..., n-2 \\
\dfrac{\partial R}{\partial t} + \dfrac{\partial}{\partial x}\left(u_n R - \dfrac{(u_n - u_{n-1})^2}{2} + \varphi_{n-1} - \dfrac{\beta_n h_n^2}{2}\Big(\dfrac{\partial u_n}{\partial x}\Big)^2\right) = f_n - f_{n-1},
\end{cases}
$$

where

$$
K = u_1 - u_2 - \frac{\beta_1}{3h_1}\frac{\partial}{\partial x}\left(h_1^3 \frac{\partial u_1}{\partial x}\right), \; R = u_n - u_{n-1} - \frac{\beta_n}{3h_n}\frac{\partial}{\partial x}\left(h_n^3 \frac{\partial u_n}{\partial x}\right).
$$

Here

$$
h_n = H - \sum_{j=1}^{n-1} h_j, \quad \varphi_i = -(b_{i+1} - b_i)\sum_{j=1}^{i} h_j.
$$

Stationary solutions

For the class of stationary solutions the first n equations of (1) yield

$$u_i h_i = Q_i = \mathrm{const}.$$

Let us take $Z = \mathrm{const}$, $f_i = 0$ and, for simplicity $\beta_1 = 0$, $\beta_n = 1$. Then we have the following ODEs for h_i and p:

$$\begin{aligned} &-\frac{Q_i^2}{h_i^3} h_i' + p_i' = 0, \quad i = 1, ..., n-1 \\ &-\frac{Q_n^2}{h_n^3} h_n' + p_n' + \frac{Q_n^2}{3h_n}\left(h_n'' - \frac{h_n'^2}{h_n}\right)' = 0, \end{aligned} \tag{2}$$

where

$$p_1 = p, \quad p_i = p + \sum_{j=1}^{i-1} (b_j - b_i) h_j.$$

Let us transform this system to the normal form. Expressing p_1' from the first equation (2) and using the math induction, it can be shown that

$$h_k' = \alpha_k h_1', \quad k = 2, ..., n-1$$

$$\alpha_2 = \left(\frac{Q_1^2}{h_1^3} - b_2\right)\frac{h_2^3}{Q_2^2}, \quad \alpha_k = \left(\frac{Q_1^2}{h_1^3} - b_k + \sum_{j=2}^{k-1} \alpha_j (b_j - b_k)\right)\frac{h_k^3}{Q_k^2}.$$

Considering that the total depth H is constant and $p' = Q_1^2 h_1' / h_1^3$, we have

$$h_1' = -G h_n', \quad p_n' = F h_n',$$

$$G = \left(1 + \sum_{k=2}^{n-1} \alpha_k\right)^{-1}, \quad F = b_n - \left(\frac{Q_1^2}{h_1^3} + \sum_{j=2}^{n-1} \alpha_j b_j\right) G.$$

Finally, the normal form of system (2) is

$$h_1' = -Gr, \quad h_k' = -\alpha_k G r, \quad k = 2, ..., n-1$$

$$h_n' = r, \quad r' = s, \quad s' = \left(\frac{3 - r^2}{h_n^2} - \frac{3 F h_n}{Q_n^2} + \frac{2s}{h_n}\right) r. \qquad (*)$$

Bifurcation of constant flow. Let us construct a non-trivial solution of ODEs (2) that is continuously adjacent to constant flow

$$h_i = h_i^0, \quad u_i = u_i^0, \quad i = 1, ..., n$$

as $x \to -\infty$. We linearize Eqs. $(*)$. System for small perturbations is

$$\tilde{h}_k' = -\alpha_k^0 G^0 \tilde{r}, \quad \tilde{h}_n' = \tilde{r}, \quad \tilde{r}' = \tilde{s}, \quad \tilde{s}' = 3\tilde{r}\left(\frac{1}{(h_n^0)^2} - \frac{F^0 h_n^0}{(Q_n^0)^2}\right).$$

We are looking for the solutions of this system in the form

$$(\tilde{h}_i, \tilde{r}, \tilde{s}) = (\hat{h}_i, \hat{r}, \hat{s}) \exp(\nu x),$$

where $\hat{h}_i$, $\hat{r}$, and $\hat{s}$ are the amplitudes, and ν is a positive parameter. If

$$\nu^2 = \frac{3}{(h_n^0)^2}\left(1 - \frac{F^0 (h_n^0)^3}{(Q_n^0)^2}\right)$$

then $\hat{h}_n$ can be set arbitrary and the remaining amplitudes are

$$\hat{r} = \nu \hat{h}_n, \quad \hat{s} = \nu^2 \hat{h}_n, \quad \hat{h}_k = -\alpha_k^0 G^0 \hat{h}_n, \quad i = k, ..., n-1.$$

Soliton-like solutions. We take $h_1^0 = 0.1$, $h_6^0 = 0.7$, $h_2^0 = \ldots = h_5^0 = 0.05$, and $b_i = (i-1)/5$, $i = 1, \ldots 6$. Top panel: $u_i^0 = U = 0.45$ (no shear).

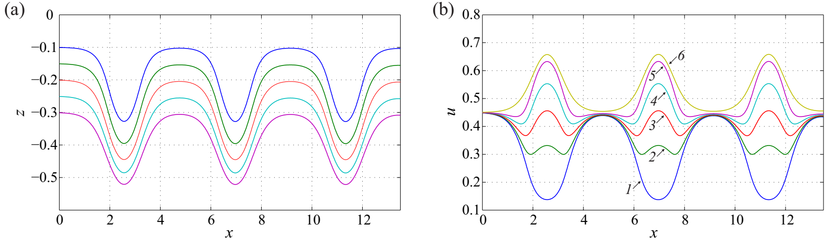

Bottom panel: $u_i^0 = U(1 + \omega(6-i)/5)$; (a) $\omega = -0.1$, (b) $\omega = 0.035$.

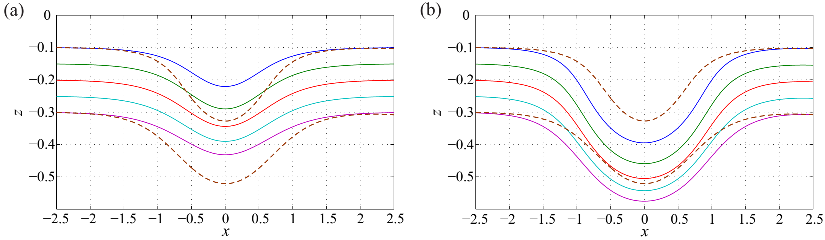

Wind-driven internal waves

Wind-driven IWs in a closed reservoir ($L = 20\,\text{km}$, $H = 400\,\text{m}$). At $t = 0$ the fluid is at rest and the pycnocline is located at a depth of 10 to 20 meters. The temperature varies from 12° C in the top layer to 4.5° C in the bottom layer. Friction velocity: $u_*^2 = C_D \rho_a V^2/\rho_1$, $C_D = 1 \div 1.5 \cdot 10^{-3}$ (Wuest & Lorke, 2003); $\rho = \rho(T)$ according to (Chen & Millero, 1986). 7-layer model; at $t = 0$: $h_1 = 10$, $h_i = 2$, $h_7 = 380\,\text{m}$; $b_7 = 0.0046\,\text{m/s}^2$.

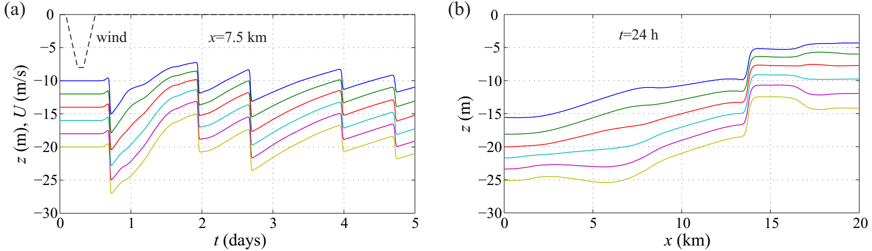

(a) interfaces $z = z_i(t)$ at $x = 7.5\,\text{km}$ over 5 days (solid curves) and wind speed V (dashed curve); (b) interfaces $z = z_i(x)$ at $t = 24\,\text{h}$.

IWs generated by gusty wind

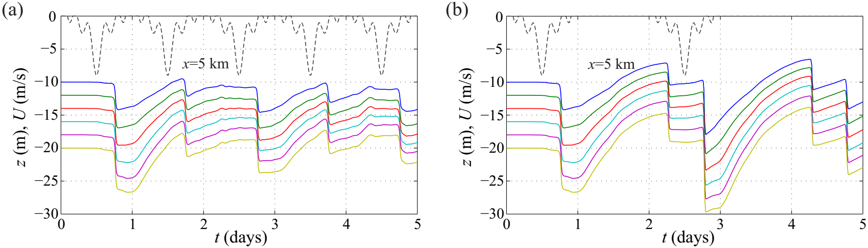

(a) interfaces $z = z_i(t)$ at $x = 5\,\mathrm{km}$ over 5 days (solid curves) and wind speed V (dashed curve); (b) the wind blows only on the first and third days.

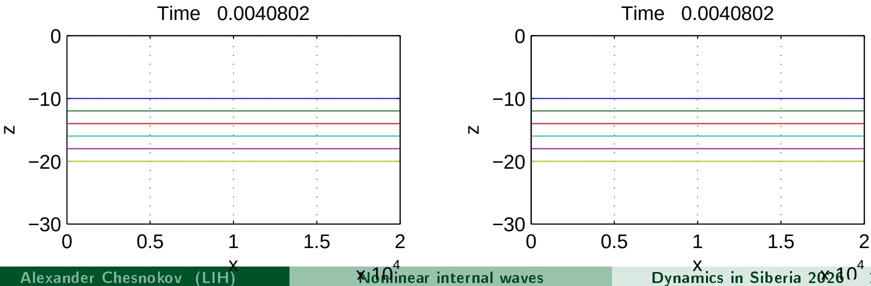

Field observations

Full-scale experiment with drifters: South Baikal, water area near the village Bolshiye Koty, Zhdanov, 2014; Aslamov et al., Limnological Institute.

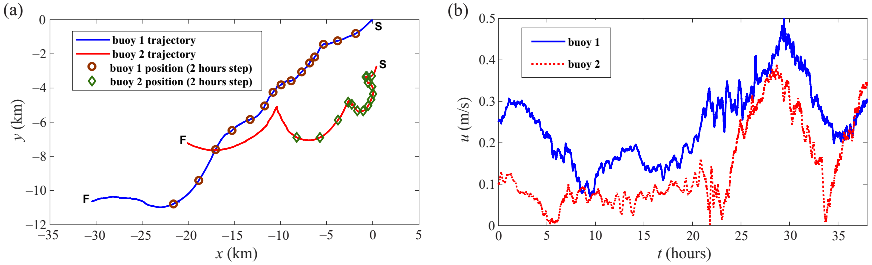

Two free-floating buoys: (a) trajectories of Buoys 1 and 2 (the first 30 hours); (b) modulus of the buoys' velocity. Each buoy was equipped with a vertical thermistor string with 14 sensors located at equal distances from each other at depths from 10 to 31 m below the free surface. Temperature at these depths in the range of 5–11°C (August 31, 2009).

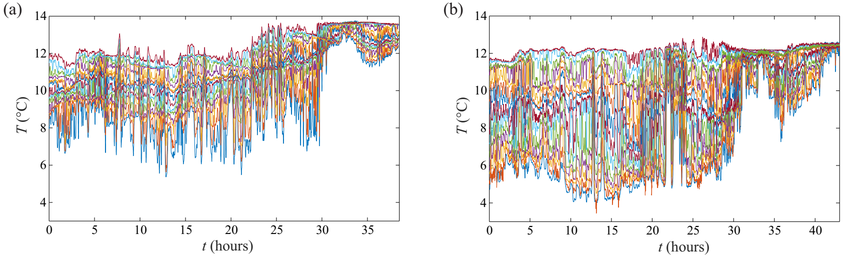

Temperature (5–11°C) at fixed horizons on time: (a) Buoy 1; (b) Buoy 2.

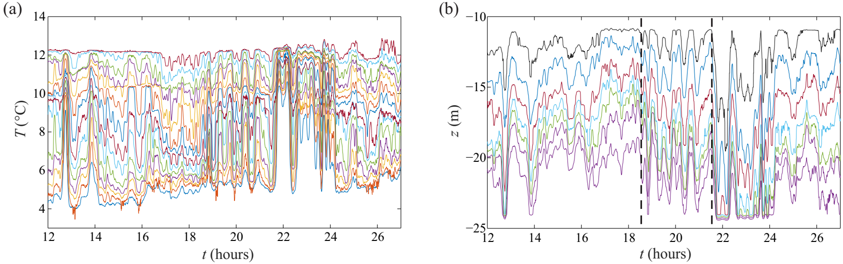

(a) fragment of (b) from the top panel; (b) isotherms with a step of 1°C.

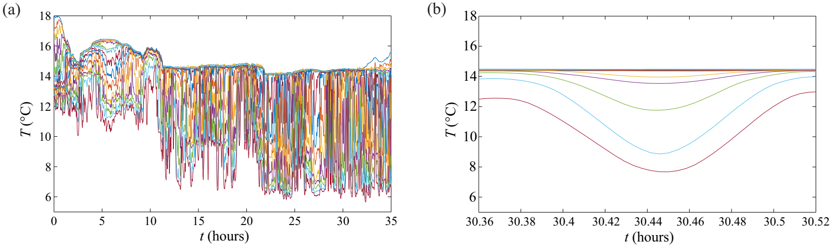

Temperature at depths from 0.75 m to 10.5 m in July 2025, obtained by a floating buoy near neutrino telescope (top panel). IWs recorded by a moored buoy in coastal waters ($H = 34$ m) in Sept. 2024 (bottom panel).

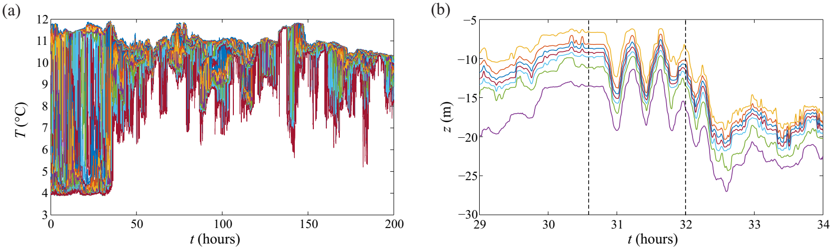

Comparison with simulation results

Quasi-periodic waves in the coastal zone. Data from the previous figure ($H = 34$ m); 8-layer model (2). At $x = 0$: $h_1 = 6.64$, $h_2 = 1.54$, $h_3 = h_4 = h_5 = 0.53$, $h_6 = 1.36$, $h_7 = 2.40$, $h_8 = 20.48$ m; $u_i = \mathrm{Fr}\sqrt{bH}$; $b = 0.0041 \mathrm{m/s}^2$; $\mathrm{Fr} = 0.472$ (selected based on the wave amplitude). Transition to time: $t = (x/\bar{D})/60^2 + t_0$, here $\bar{D} = 0.66\,D$, $D = 0.176$ m/s.

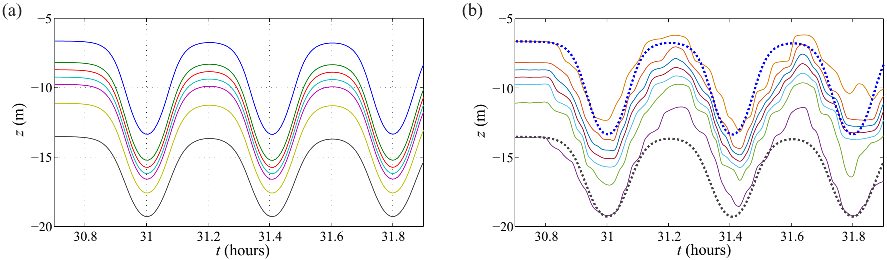

(a) solution of ODEs (2) for $n = 8$; (b) isotherms in the range of 5–11°C are shown by solid, dotted lines – upper and lower curves in panel (a).

IWs in the deep-water region. At $x = 0$: $h_1 = 11$, $h_2 = 2$, $h_3 = 3$, $h_4 = 1.75$, $h_5 = 1$, $h_6 = 1.75$, $h_7 = 3.5$, $h_8 = 176$ ($H = 200\,\mathrm{m}$); $b = 0.0041\,\mathrm{m}/s^2$; $V = 0.1\,\mathrm{m/s}$ (velocity in the upper layer); $\mathrm{Fr} = 0.195$, $D = 0.176\,\mathrm{m/s}$ (according to the wave amplitude); $u_i = D + V(n - i)/7$ (shear flow). Transition to time as before with $\bar{D} = D$.

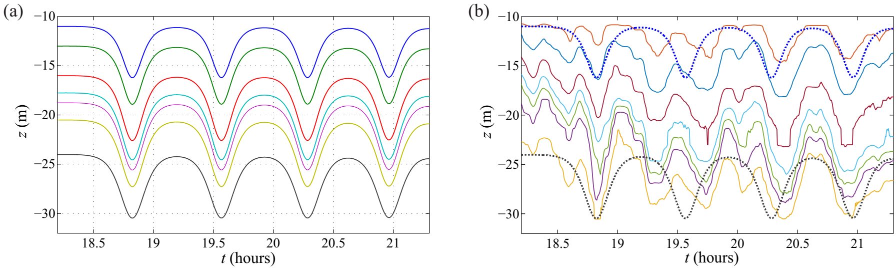

(a) quasi-periodic solution of Eqs. (2) with $n = 8$ under field condition for Buoy 2; (b) isotherms (solid curves), dots indicate the internal boundaries of the outer layers.

IWs with a trapped core (near-surface solitary wave of elevation). To construct such a wave, we assume that the lower boundary of the thermocline acts as a solid boundary. Data: floating buoy, July 2025. We take 6-layer model; at $x = 0$: $h_1 = 9.68$, $h_2 = 0.39$, $h_3 = h_4 = h_5 = 0.14$, and $h_6 = 0.51\,\mathrm{m}$ ($H = 11\,\mathrm{m}$); $\mathrm{Fr} = 0.375$, $D = 0.087\,\mathrm{m/s}$, $V = 0.046\mathrm{m/s}$. This choice of the Froude number and velocity shear ensures agreement.

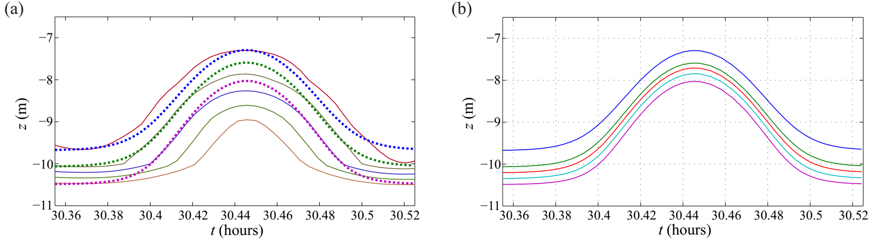

Near-surface solitary wave of elevation: (a) isotherms in the range from 9 to 13°C (solid lines), dots show several interfaces obtained using the model; (b) solution of the model for $n = 6$ in the form of a traveling wave.

Conclusion

We focused on demonstrating the capabilities of model (1) to describe nonlinear internal waves in a stratified fluid.

- In the class of traveling waves, soliton-like and quasi-periodic solutions adjacent to a shear multilayer flow are constructed. It is shown that a positive velocity shear increases the amplitude and wavelength, while a negative shear decreases them.
- We conducted calculations of the IWs propagation and seiche oscillations in a large stratified reservoir and show that winds classified as fresh breezes can generate IWs with amplitudes greater than 10 m.
- We processed a series of available data on temperature fluctuations in South Baikal, obtained using free-floating and moored buoys, and presented them in the form of isotherms.
- It is shown that the model is capable of correctly describing the observed wave packets.

THANK YOU FOR ATTENTION !